View metadata, citation and similar papers at core.ac.uk

brought to you by CORE

provided by Kanazawa University Repository for Academic Resources

Influence of applied tensile stress on formation and growth of ellipsoidal ω precipitates in a Ti-20wt%Mo alloy

著者	Monzen Ryoichi, Kawai Ryutaro, Watanabe Chihiro
journal or publication title	PTM 2015 - Proceedings of the International Conference on Solid-Solid Phase Transformations in Inorganic Materials
number	2015
page range	427-434
year	2015-07-03
URL	http://hdl.handle.net/2297/45569

INFLUENCE OF APPLIED TENSILE STRESS ON FORMATION AND GROWTH OF ELLIPSOIDAL ω PRECIPITATES IN A Ti-20wt%Mo ALLOY

Ryoichi Monzen, Ryutaro Kawai, Chihiro Watanabe

Division of Mechanical Science and Engineering, Graduate School of Natural Science and Technology, Kanazawa University, Kakuma-machi, Kanazawa 920-1192, Japan

Keywords: Ti-Mo alloy, ω precipitates, nucleation, growth, tensile stress, interaction energy

Abstract

The effects of tensile stress on the nucleation and growth of ellipsoidal ω phase precipitates have been investigated for a Ti-20wt%Mo alloy aged at 300 °C. Application of a tensile stress promotes not only the nucleation but also the growth of ω precipitates. Estimates of the average misfit strains along the loading and the transverse directions from measurements of the length change reveal the preferential formation of specific ω variants among the four crystallographically-equivalent variants. The average size of the precipitates in the alloy aged under no stress follows initially a parabolic growth law, whereas when aged under a tensile stress of 400 and 450MPa the precipitate size increases linearly with aging time, this fact indicating that while the growth of ω precipitates is governed by diffusion of Mo from the ω/β interface to the β matrix under no stress, precipitate growth is instead interface-controlled under tensile stress.

Introduction

The influence of a directional stress during aging on the orientation distribution of precipitate structures has been examined widely for Al-Cu system alloys [1-3] and Cu-Be system alloys [4, 5]. For example, Monzen et al. [4] have shown by transmission electron microscopy (TEM) that application of an external stress during aging at 200 °C induces the oriented precipitation of disk-shaped GP zones in single crystals of a Cu-0.9Be alloy (All compositions in this text are expressed by weight per cent, wt%). The disk-shaped GP zones consist of monolayers of Be atoms on the $\{100\}_\alpha$ planes. A compressive stress along the $[001]_\alpha$ direction assists preferential formation of the GP zones perpendicular to the stress axis and tensile stress induces the same parallel to the stress axis. Moreover, Monzen et al [5] have examined the effects of an external stress on the nucleation and growth of disk-shaped γ" phase for a Cu-1.2Be-0.1Co alloy aged at 320 °C. The metastable γ" phase is composed of alternate Be and Cu matrix layers parallel to the $\{100\}_\alpha$ planes. A compressive stress applied in the [001] direction during aging preferentially accelerates the nucleation and growth of the γ" variant normal to the [001] axis among the three crystallographically-equivalent variants. However, a tensile stress does not significantly affect the nucleation and growth of γ" precipitates. The acceleration of the nucleation and growth of the specific γ" variants can be understood through the interaction energy between the stress acting on the γ" variants and their misfit strains.

Nishizawa et al. [6] have measured the number of ω precipitates in constant areas in Ti-20Mo alloy specimens aged at 350 °C under no stress and an applied tensile stress of 413 MPa, and concluded that a tensile stress applied during aging promotes the nucleation of ω precipitates. Since the ω precipitates have an ellipsoidal shape slightly elongated along $<111>_\beta$ of the β-Ti

matrix [7], in contrast to the disk-shaped GP zones and γ" phase in Cu-Be alloys [4, 5] and the disk-shaped GP[1] zones and θ' phase in Al-Cu alloys [1-3], it is interesting to examine how applied external stress affects the formation of the four crystallographically-equivalent ω variants and the growth of ω precipitates. We have found the stress-oriented nucleation of the ω precipitates, and furthermore found the change from the diffusion-controlled growth of ω precipitates under no stress to the interface-controlled growth under tensile stress, as will be shown later.

Experimental

Ingots of a Ti-20Mo alloy were prepared by non-consumptive arc melting. The ingots were cut into sheets, cold-rolled to a 50% reduction in thickness and then spark-cut into specimen strips. The specimens had a cross-section of 1 mm × 5 mm and a gage length of 20 mm. They were solution-treated at 950 °C for 2 h in a vacuum and quenched into water. The solution treatment also caused complete recrystallization of the specimens. The solution-treated specimens were then aged at 300 °C for various times either under an applied tensile stress of 450 MPa (stress aging) or under no stress (free aging). The applied stress of 450 MPa is about three fourths of the yield strength of the solution-treated specimen at 300 °C. Also the solutionized specimens were free-aged (FA) at 300 °C for 3 h and then aged at 300 °C under an applied tensile stress of 300, 400 and 450 MPa, or FA at 300 °C for 3 h and then FA at 300 °C for various times.

Length changes ε_T on aging were examined by measuring, with a micrometer, the distance between two scribed marks, about 8 mm apart for the specimens tensile-stress-aged at 300 °C for 3 h and then FA at 350 °C for various times, or FA at 300 °C for 3 h and then FA at 350 °C for various times. The length change is defined as $\varepsilon_T=(l-l_0)/l_0$, where l_0 and l are the length between the two marks before and after aging, respectively. The measurement accuracy of length change is in the order of 10^{-5} in strain. An X-ray analysis was performed to measure the lattice parameters of the solution-treated and aged specimens.

Thin foils, 0.2 mm thick, for TEM observations were prepared by grinding the aged specimens with SiC papers and by electropolishing using a solution of 60 vol% methanol, 35 vol% 2-Butoxyethanol and 5 vol% perchloric acid at −20 °C and 15 V in a twin-jet electropolisher. Microscopy was performed using a JEOL 2010FEF microscope operated at 200 kV.

Results and Discussion

External Stress Effect on Nucleation

Figure 1(a) shows a dark-field TEM image of the Ti-20Mo specimen aged at 300 °C for 12 h under a tensile stress of 450 MPa. Figure 1(b) is the corresponding $[011]_\beta$ selected-area diffraction pattern (SADP). Reflections due to two ω variants, I and II, are present out of the four possible crystallographically-equivalent ω variants. The dark-field image was acquired using a reflection due to the variant II. The variants I and II aligned with the β-Ti matrix according to the following orientation relationship: $[1\bar{1}1]_\beta // [0001]_{\omega I}$; $(\bar{2}\bar{1}1)_\beta // (10\bar{1}0)_{\omega I}$; $(011)_\beta // (\bar{1}2\bar{1}0)_{\omega I}$ and $[\bar{1}\bar{1}1]_\beta // [0001]_{\omega II}$; $(2\bar{1}1)_\beta // (1\bar{1}00)_{\omega II}$; $(011)_\beta // (11\bar{2}0)_{\omega II}$. The variant I and II had an ellipsoidal shape elongated along $[1\bar{1}1]_\beta$ and $[\bar{1}\bar{1}1]_\beta$ on $(011)_\beta$. Here, the shape of ω precipitates is assumed to be a spheroid described in the x-y-z coordinates by $x^2/(w/2)^2+y^2/(w/2)^2+z^2/(l/2)^2 \leq 1$.

Figures 2(a), (b) and (c) display the number density N of the ellipsoidal ω precipitates, the lattice parameter of the β-Ti matrix measured by X-ray analysis, and the average precipitate diameter d as a function of aging time t for the specimens aged at 300 °C under a tensile stress of 450 MPa

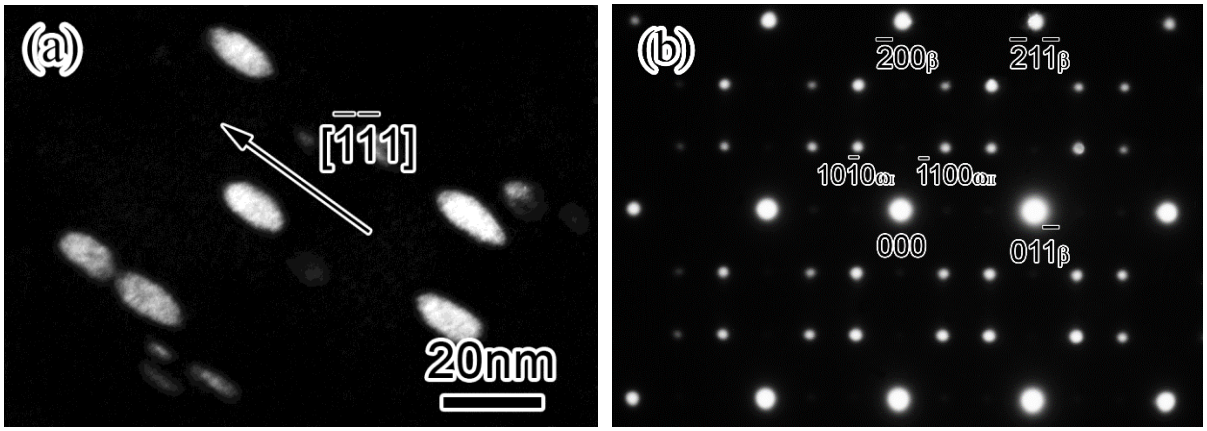

Figure 1. (aDark-field TEM image of ω precipitates in a Ti-Mo specimen aged at 300 °C for 12 h under a tensile stress of 450 MPa. (b) $[011]_\beta$ SADP corresponding to (a).

and free-aged (FA) at 300 °C. The number density of ω precipitates is defined as the volume fraction of precipitates divided by the average volume of a single precipitate. The volume fraction was determined by applying the lattice parameters of the tensile-stress-aged (TSA) and FA specimens to the experimental data reported for the dependence of the lattice parameter on the Mo concentration ($\Delta a = -0.0002$ nm/at%) in the literature [8], and using the lattice parameters of $a = 0.2820$ nm and $c = 0.4606$ nm for the ω phase with a hexagonal structure [9]. The concentration of Mo in the ω precipitates is assumed to be 10wt% equal to the equilibrium concentration of Mo at 300 °C in the Ti-Mo binary phase diagram [10]. Even if the Mo concentration in the precipitates is assumed to be 20wt% equal to the Mo concentration in the present alloy, the volume fraction estimated at each aging time is not significantly affected. The average volume of an ellipsoidal precipitate was obtained by measuring w and l of the ω precipitates. Then the diameter d of a sphere having the same volume fraction as the ellipsoidal precipitate was calculated.

Figure 2(a) shows that the number density of ω precipitates is constant over a time span of 1.5h (5.4×10^3 s) in the case of the TSA specimen, and over 3 h for the FA specimens. Thus the formation of the ω precipitates in the TSA and FA specimens is completed after 1.5 and 3h. More importantly, the number density of ω precipitates in the TSA specimen is higher than that in the FA specimen, indicating that the formation of ω precipitates is aided by applied tensile stress. In Fig. 2(b), the lattice parameter decreases with increasing aging time for the two specimens. Diffusion of Mo atoms in ω precipitates from the ω/β interface to the β-Ti matrix occurs as the ω precipitates grow [10]. Since the size of Mo atoms is smaller than that of Ti atoms, the increase in Mo atoms within the β-Ti matrix causes the decrease in the lattice parameter. Moreover, it can be seen from Fig. 2(c) that aging under tension accelerates the growth of the precipitates. This will be discussed in the next section.

Figure 3 presents the length change ε_T along the loading direction (LD) and transverse direction (TD), plotted as a function of aging time t for the specimen FA at 300°C for 3h and then FA at 350°C (FA-FA) and the specimen TSA (450MPa) at 300°C for 3h and then FA at 350°C (TSA-FA). The specimens TSA and FA at 300°C for 3h each exhibit a slight decrease in length change. Length change along the LD and TD for the TSA-FA and FA-FA specimens rapidly decreases and then eventually plateaus after about 53h (1.908×10^5s). The plateau value of ε_T along the LD for the TSA-FA specimen is larger than that along the TD for the same specimen. In addition, the values of ε_T measured along several directions of the specimen FA at 300°C for 3h and then FA

at 350 °C for 53 h were identical within experimental error, indicating that there was no anisotropy in length change of the FA-FA specimen.

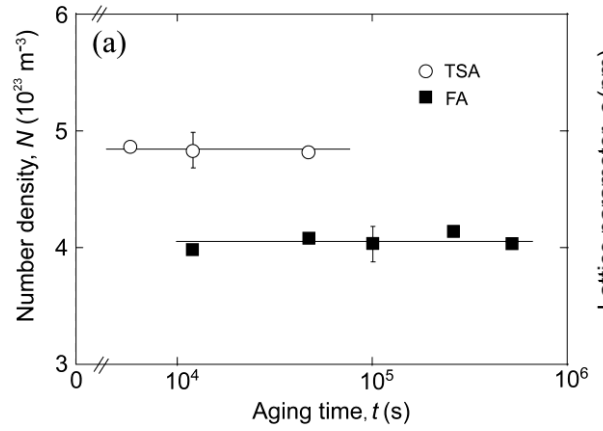

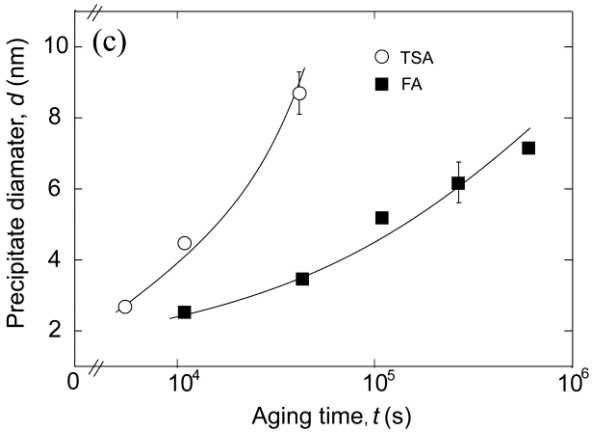

Figure 2. Aging time t dependence of (a) the number density N of ω precipitates, (b) the lattice parameter a of β-Ti matrix and (c) the average diameter d of ω precipitates in Ti-Mo specimens, TSA (450MPa) and FA at 300 °C. Representative error bars are shown.

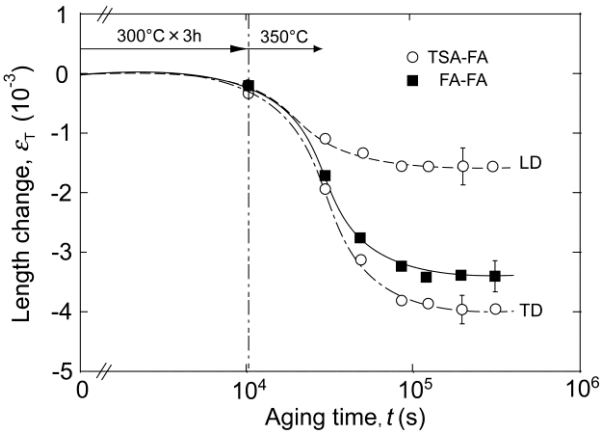

Figure 3. Aging time t dependence of the length change ε_T for Ti-Mo specimens, TSA at 300 °C for 3 h and FA at 350 °C (TSA-FA) and FA at 300 °C for 3 h and FA at 350 °C (FA-FA). Representative error bars are shown.

The specimen length-change ε_T along any direction can be written as functions of the average misfit strain ε_a along the same direction caused by the misfit strains of precipitates, the volume fraction f of the precipitates, and the dimensional change ε_l due to the increase in Mo atoms in the solid solution, as follows [11]

$$\varepsilon_T = f\varepsilon_a + (1-f)\varepsilon_l, \quad (1)$$

where $\varepsilon_l=(a-a_0)/a_0$. Here a_0 and a are the lattice parameters of the specimens before and after aging.

We are able to estimate the average misfit strains ε_{aL} and ε_{aT} along the LD and TD for the TSA-FA specimen, as well as the average misfit strain ε_{aF} for the FA-FA specimen. A value for f of 0.14 was obtained by applying the values a_0=0.3253 nm and a=0.3232 nm before and after aging at 350 °C for 53 h (Fig. 3) to the experimental data regarding the dependence of the lattice parameter on Mo concentration [8]. The Mo concentration in the ω precipitates was assumed to be 10wt%, as noted above. The values of ε_{aL}=0.028, ε_{aT} = 0.008 and ε_{aF} = 0.010 were obtained for the specimens TSA and then FA at 350 °C for 53 h (TSA-FA'), and FA and then FA at 350 °C for 53 h (FA-FA'). These values were estimated from the values of ε_T in Fig. 3, as well as from f and ε_1. The value of ε_{aF} = 0.010 is nearly identical to the value of ε_c = 0.0088 calculated by Hickman [12] from the lattice parameters of the ω precipitates and β matrix. For the TSA-FA' specimen, ε_{aT} = 0.008 < ε_{aF} = 0.010 < ε_{aL} = 0.028. This indicates that tensile stress preferentially aids the formation of specific ω variants out of the four crystallographically-equivalent variants, having positive misfit strains along the LD greater than ε_{aF} = 0.010.

The origin of the promotion of the formation of ω precipitates during aging under applied tensile stress (Fig. 2(a)), and the relationship among the average misfit strains along the LD and TD for the TSA specimen and that for the FA specimen can be understood to arise through the interaction energy between an external stress σ_{ij} and a misfit strain ε_{ij} (stress-free transformation strain). That is, the cause of the present results is understood to be due to the work done by the external stress during the nucleation of ω precipitates. The interaction energy F_I is expressed as [13]

$$F_I = -V\sigma_{ij}\varepsilon_{ij}, \tag{2}$$

where V is the volume of the ω precipitate. According to a classical nucleation theory [19], the interaction energy F_I affects the nucleation rate R as written by [14]

$$R \propto \exp\left(-\frac{\left(G^* + F_I^*\right)}{kT}\right), \tag{3}$$

where G^* is the activation energy for nucleation in absence of a stress, F_I^* is the interaction energy associated with nucleation of the ω precipitate of a critical nucleus volume, k is Boltzmann's constant and T is the absolute temperature.

Eqs. 2 and 3 predict that applied tensile stress promotes the nucleation of ω precipitates because the average misfit strain ε_{aF} = 0.010 for the FA specimen. This prediction is in agreement with the result shown in Fig. 2(a). Similarly, it may be expected from Eqs. 2 and 3 that for the TSA specimen, the average misfit strain ε_{aL} along the LD is larger than ε_{aF} = 0.010 for the FA specimen. This is the case, as described above.

External Stress Effect on growth

Figure 4 depicts dark-field images of the Ti-20Mo specimens, FA and TSA (450 MPa) at 300 °C for 12 h after free-aging at 300 °C for 3 h. These images were obtained with an incident electron beam along the $[011]_\beta$ direction. The two dark-field images were taken using two reflections due to the variant II. All the four variants had an ellipsoidal shape elongated along $<111>_\beta$ with an aspect ratio of about 2, irrespective of application of external stress. It may be noted in Fig. 4 that the precipitate sizes w and l for the TSA specimen are larger than those for the FA specimen.

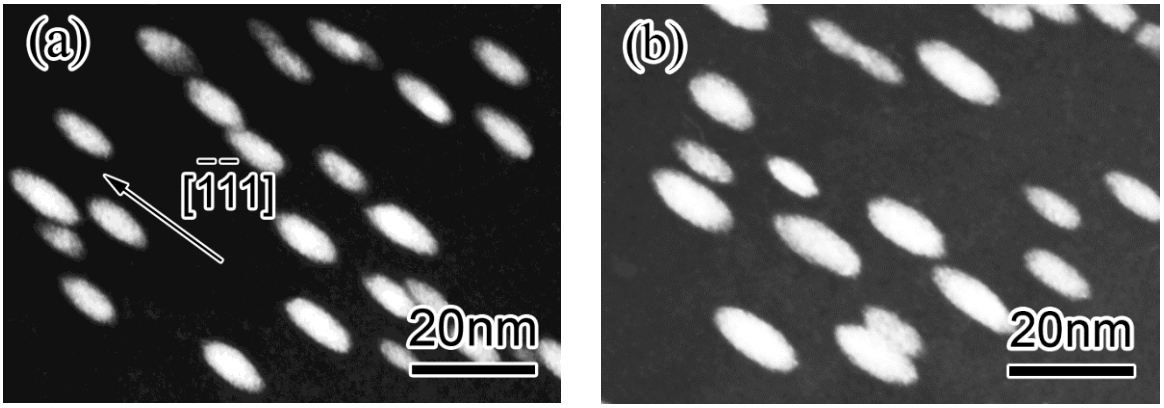

Figure 4. Dark-field TEM images of ω precipitates in Ti-Mo specimens (a) FA and (b) TSA (450 MPa) at 300 °C for 12 h after free-aging at 300 °C for 3 h. The zone axis is along $[011]_{\beta}$.

As described in the previous section, the nucleation of the ω precipitates in the specimen FA at 300 °C is completed after 3 h. The average diameter d_0 of the ω precipitates in the FA specimen was 2.7 nm. The average precipitate diameter d in the specimens FA and TSA at 300 °C after free-aging at 300 °C for 3 h was measured as a function of aging time t after aging at 300 °C for 3 h. Figure 5 displays $(d-d_0)$ against aging time t on logarithmic scales for the specimens, aged at 300 °C under no stress (TSA0), and a tensile stress of 300 (TSA300), 400 (TSA400) and 450 MPa (TSA450). It can be seen that aging under tension accelerates the growth of the precipitates. In the initial stage of aging, a linear relationship exists between log $(d-d_0)$ and log t for all the specimens. This means that $(d-d_0)$ is nearly proportional to $t^{1/n}$. From the slopes of the straight lines obtained by the least-squares method, n can be obtained and the calculated values are listed in Table 1. For the FA specimen, $n = 2.0 \pm 0.2$. This shows that the growth kinetics of ω precipitates follows a diffusion-controlled parabolic growth law [15]. It is also seen that the value of n decreases with increasing the magnitude of tensile stress and saturates to 1.0 ± 0.2. This value shows that the growth of ω precipitates under tensile stress obeys an interface-controlled growth law [15]. Consequently, while the growth of ω precipitates is governed by the diffusion of Mo atoms in ω precipitates from the β/ω interface to the β-Ti matrix [10], precipitate growth is instead interface-controlled under tensile stress.

In the interface-controlled growth of a precipitate, the interface velocity v_I is written as [16]

$$v_I = \delta\nu(-\Delta G_m / kT)\exp(-\Delta G_d / kT), \tag{4}$$

where δ is the interface width, ν is the vibrational attempt frequency, ΔG_m is the free energy change per atom and ΔG_d is the activation energy for interface transport. The interface velocity for various massive reactions has been found to obey the interface-controlled growth equation [16]. We consider that the interface velocity under an external stress σ_{ij} is expressed as

$$v_I = \delta\nu[-(\Delta G_m - \sigma_{ij}\varepsilon_{ij} / V_m) / kT]\exp(-\Delta G_d / kT), \tag{5}$$

where V_m is the molar volume of the precipitate.

Eq. 5 predicts that applied tensile stress promotes the growth of ω precipitates since the average misfit strain $\varepsilon_{aF} = 0.010$ for the FA specimen. This prediction is in agreement with the result shown in Fig. 5.

To quantitatively substantiate Eq. (5), a further investigation of the dependence of the growth velocity of ω precipitates on the magnitude of external stress and ageing temperature will be required. The investigation is now in progress.

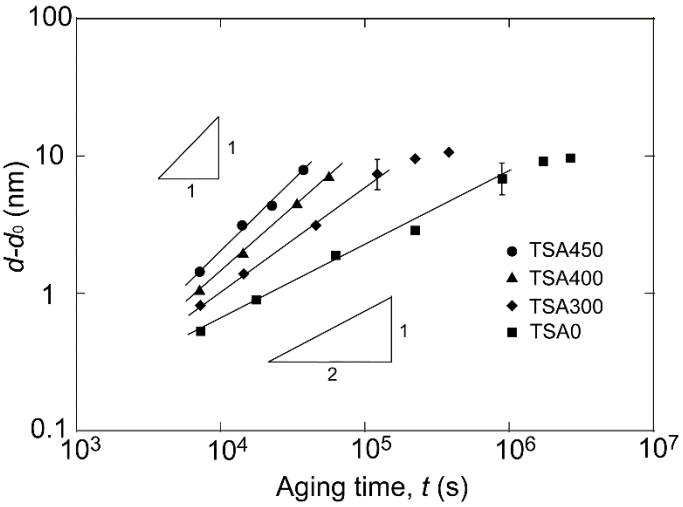

Figure 5. Variation in $(d-d_0)$ of ω precipitates with aging time t for Ti-Mo specimens, aged at 300 °C under no stress (TSA0) and a tensile stress of 300 (TSA300), 400 (TSA400) and 450 MPa (TSA450). Representative error bars are shown.

Table 1 Calculated n value for each specimen.

Specimen	TSA0	TSA300	TSA400	TSA450
n	2.0	1.5	1.0	1.0

Conclusions

(1) Application of tensile stress during aging at 300 °C promotes the nucleation and growth of ellipsoidal ω precipitates in a Ti-20wt%Mo alloy.

(2) From measurements of the length change, the average misfit strains along the loading and the transverse directions, caused by the misfit strains of ω precipitates, have been estimated for the tensile-stress-aged alloy. The estimates reveal that specific ω variants among the four crystallographically-equivalent variants are preferentially formed.

(3) The average size of the precipitates in the alloy aged under no stress follows initially a parabolic growth law, whereas when aged at 300 °C under a tensile stress of 400 and 450 MPa the precipitate size increases linearly with aging time. This indicates that the growth of ω precipitates is governed by diffusion of Mo from the ω/β interface to the β matrix under no stress, but is interface-controlled under tensile stress.

References

1. T. Eto, A. Sato and T. Mori, "Stress-oriented precipitation of G. P. Zones and θ' in an Al-Cu alloy," *Acta Metal*, 26 (1978), 499-508.
2. B. Skrotzki, G.J. Shiflet and E.A. Starke Jr, "On the effect of stress on nucleation and growth of precipitates in an Al-Cu-Mg-Ag alloy," *Metall Mater Trans A*, 27A (1996), 3431-3444.
3. A.W. Zhu and E.A. Starke Jr, "Stress aging of Al–xCu alloys: experiments," *Acta Mater*, 49 (2001), 2285-2295.

4. R. Monzen, C. Watanabe, T Seo and T. Sakai, “Effect of applied stress on precipitation of Guinier–Preston zones in a Cu–0.9 wt.% Be single crystal,” *Phil Mag Lett*, 85 (2005), 603-612.
5. R. Monzen, S. Okawara and C. Watanabe, “Stress-assisted nucleation and growth of γ″and γ′ precipitates in a Cu–1.2 wt%Be–0.1 wt%Co alloy aged at 320°C,” *Phil Mag*, 92 (2012), 1826-1843.
6. H. Nishizawa, E. Sukedai, W. Liu and H. Hashimoto, “Effect of applied stress on formation of ω-Phase in β-Ti alloys,” *Mater Trans JIM*, 39 (1998), 609-612.
7. D.D. Fontaine, N.E. Paton and J.C. Williams, “The omega phase transformation titanium alloys as an example of displacement controlled reactions,” *Acta Metall*, 19 (1971), 1153-1162.
8. S. Kun, Y. Xuezhong, W. Erdong, C. Dongfeng and G. Cheng, “Neutron diffraction study of the deuterides of Ti-Mo alloys,” *Physica B*, 385-386 (2006), 141-143.
9. J.M. Silcock, “An X-ray examination of the ω phase in TiV, TiMo and TiCr,” *Acta Metall*, 6 (1958), 481-493.
10. D.D. Fontaine, “Simple models for the omega phase transformation,” *Metall Trans A*, 19A (1988), 169-175.
11. C. Watanabe, T. Sakai and R. Monzen, “Misfit strains of precipitated phases and dimensional changes in Cu–Be alloys,” *Phil Mag*, 88 (2008), 1401-1410.
12. B.S. Hickman, “Omega phase precipitation in alloys of titanium with transition Metals,” *Trans Metall Soc AIME*, 245 (1969), 1329-1336.
13. J.D. Eshelby, “The determination of the elastic field of an ellipsoidal inclusion, and related problems,” *Proc R Soc A*, 241 (1957), 376-396.
14. M. Volmer and A. Weber, “Keimildung in ubersattigetn gebilden,” *Z Phys Chem*, 119 (1926), 277-301.
15. J.W. Christian, *The theory of Transformation in Metals and Alloys*, 3rd ed (Oxford: Pergamon Press, 2002), 480.
16. H.I. Aaronson, M. Enomoto and J.K. Lee, *Mechanisms of Diffusional Phase Transformations in Metals and Alloys* (New York, NY: Chemical Rubber Company Press, 2010).